# Metformin enhances the antitumor activity of oncolytic herpes simplex virus HF10 (canerpaturev) in a pancreatic cell cancer subcutaneous model
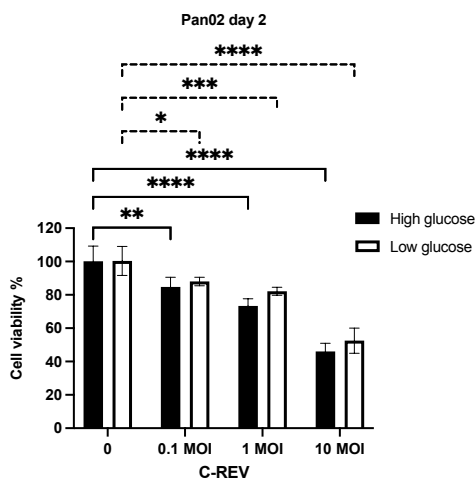
Mohamed Abdelmoneim, Ibrahim R. Eissa, Mona Al Hussein Mostafa Aboalela, Yoshinori Naoe, Shigeru Matsumura, Patricia A. Sibal, Itzel Bustos-Villalobos, Maki Tanaka, Yasuhiro Kodera & Hideki Kasuya

Supplementary Figure 1. Metformin does not enhance cell cytotoxicity induced by C-REV *in vitro*.
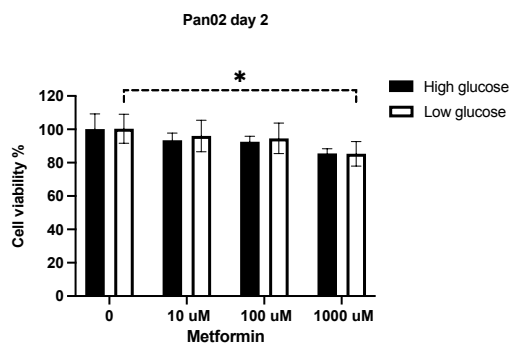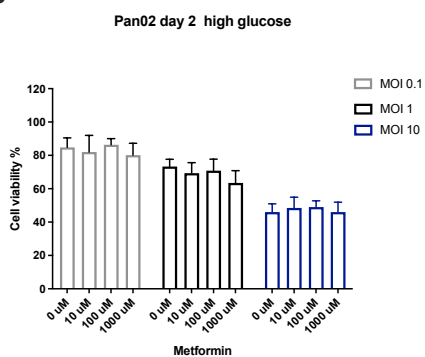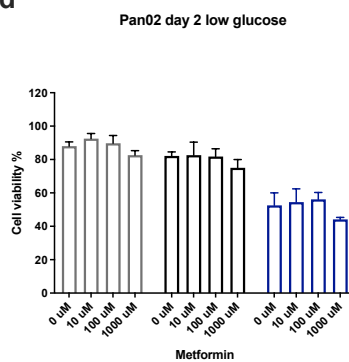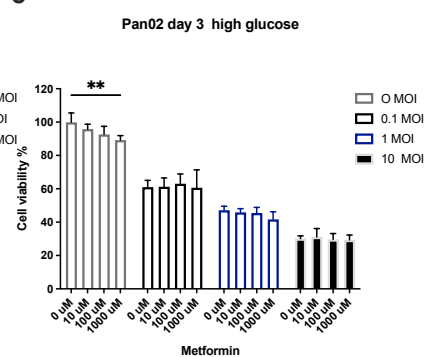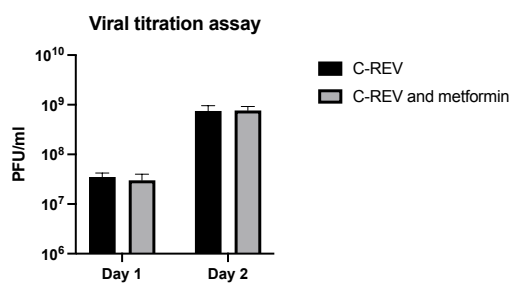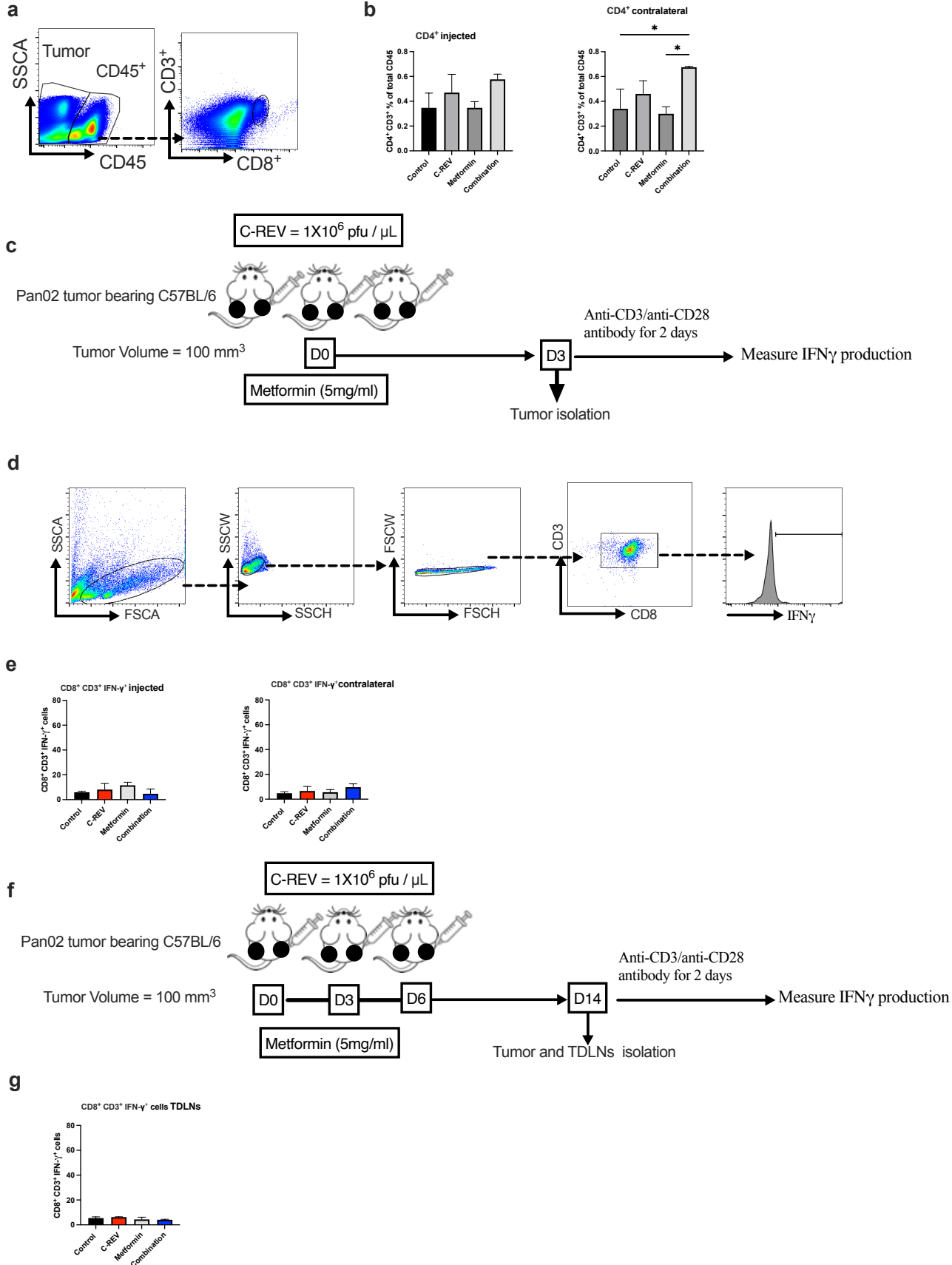
Supplementary Figure 1. Metformin does not enhance cell cytotoxicity induced by C-REV *in vitro*.
(a) Cytotoxicity of Pan02 after treatment with different concentrations of metformin (0, 10 uM, 100 uM, 1 mM) in medium containing high and low glucose (25 mM and 5.5 mM) for 2 days was determined by MTT assay. **(b)** Cytotoxicity of Pan02 after treatment with different MOI (0, 0.1, 1 and 10 MOI) of C-REV in medium containing high and low glucose for 2 days was determined by MTT assay. **(c, d)** Cytotoxicity of Pan02 after treatment with metformin and infected with several MOI of C-REV in medium containing high (c) and low (d) glucose for 2 days was determined by MTT assay.

(e) Cytotoxicity of Pan02 after treatment with metformin and infected with several MOI of C-REV in medium containing high glucose for 3 days was determined by MTT assay. Data are presented as mean ± SD (n=6). Each experiment was coducted at least three times, yielding similar results. Two-way ANOVA followed by Tukey's multiple comparisons tests was performed. **(f)** *In vitro* replication of C-REV (MOI 1) over a 2-day peroid, co-incubated with 100 uM of metformin, as assessed by viral titer. Data are presented as mean ± SD (n=3). * $p < 0.05$, ** $p < 0.01$, *** $p < 0.001$, **** $p < 0.0001$.

Supplementary Figure 2. Combination therapy does not increase IFN-γ production from CD8$^+$ CD3$^+$ TILs at day 3.

a

b

CD4$^+$ injected

CD4$^+$ contralateral

c

C-REV = 1X10^6 pfu / μL

Pan02 tumor bearing C57BL/6

Tumor Volume = 100 mm^3

D0

Metformin (5mg/ml)

D3

Tumor isolation

Anti-CD3/anti-CD28 antibody for 2 days

Measure IFNγ production

d

e

CD8$^+$ CD3$^+$ IFN-γ$^+$ injected

CD8$^+$ CD3$^+$ IFN-γ$^+$ contralateral

f

C-REV = 1X10^6 pfu / μL

Pan02 tumor bearing C57BL/6

Tumor Volume = 100 mm^3

D0   D3   D6

Metformin (5mg/ml)

D14

Tumor and TDLNs isolation

Anti-CD3/anti-CD28 antibody for 2 days

Measure IFNγ production

g

CD8$^+$ CD3$^+$ IFN-γ$^+$ cells TDLNs

Supplementary Figure 2. Combination therapy does not increase IFN-γ production from CD8$^+$ CD3$^+$ TILs at day 3. (a) Gating strategy for detection of CD8$^+$ CD3$^+$ and CD4$^+$ CD3$^+$ TILs. **(b)** Bar graphs show the percentage CD4$^+$ CD3$^+$ cells on the injected and contralateral sides. **(c)** A scheme shows schedule of C-REV and metformin treatment in C57BL/6 tumor-bearing mice for 3 days. **(d)** Gating strategy for detection of IFN-γ production from CD8$^+$ CD3$^+$ TILs. **(e)** Bar graphs show the percentage of IFN-γ production from CD8$^+$ CD3$^+$ cells on the injected and contralateral sides. **(f)** A scheme shows the schedule of C-REV and metformin treatment in C57BL/6 tumor-bearing mice for 14 days. **(g)** A bar graph shows the percentage of IFN-γ production from CD8$^+$ CD3$^+$ cells in TDLNs. Data are presented as mean ± SD (n=3 mice). One-way ANOVA with a post-hoc Tukey's tests was performed.

Supplementary Figure 3. Effect of combination therapy on T cell population in tumors and TDLNs.
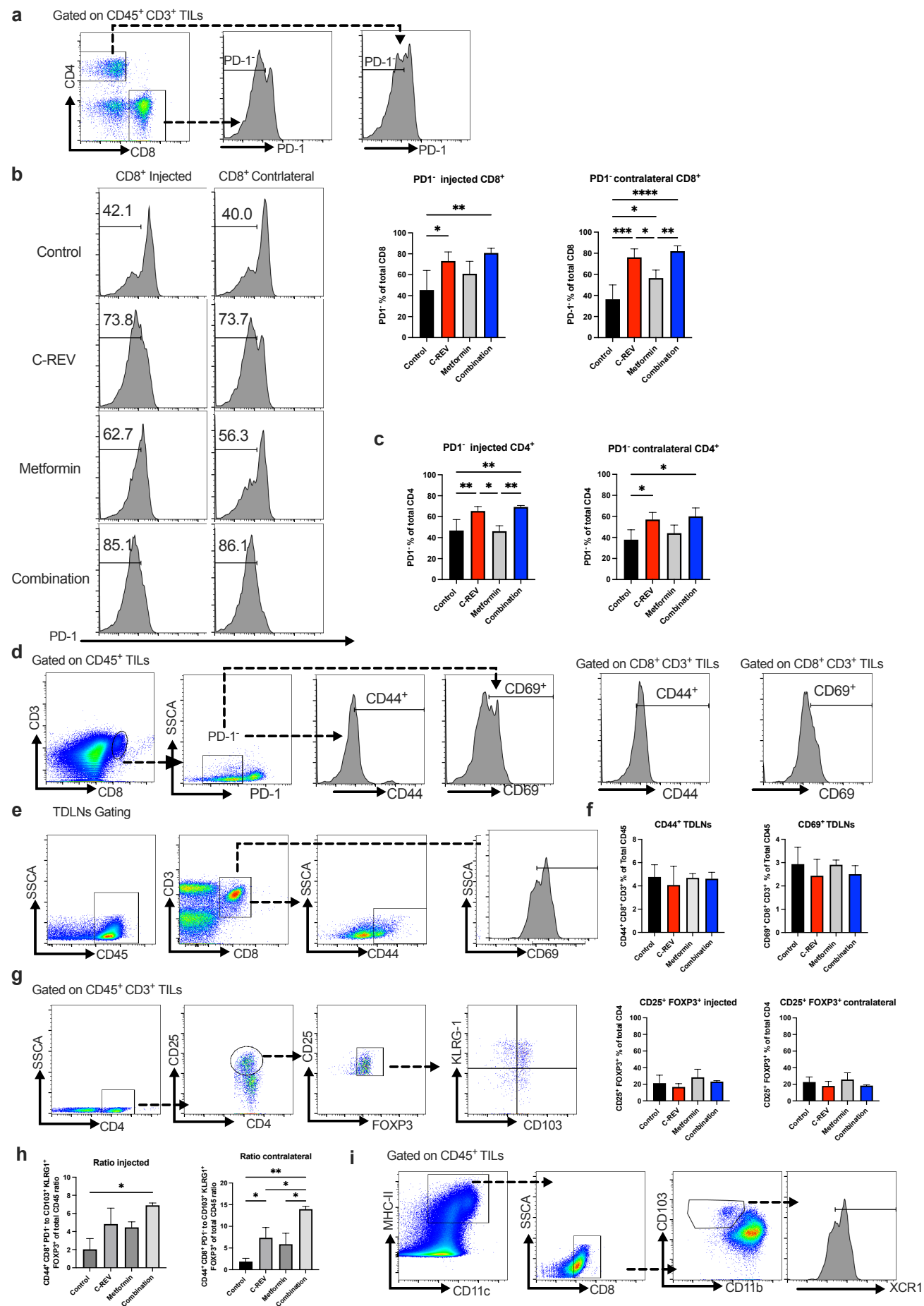
Supplementary Figure 3. Effect of combination therapy on T cell population in tumors and TDLNs. Mice were inoculated with Pan02 tumors as in Fig. 1A, tumors, and TDLNs were collected as previously shown. **(a)** Gating strategy for detection of PD-1$^-$ expression on CD8$^+$ and CD4$^+$ TILs. **(b)** Representative histograms show PD-1$^-$ expression on CD8$^+$ TILs cells on the injected and contralateral sides and bar graphs show percentage of PD-1$^-$ expression on CD8$^+$ TILs cells on the injected and contralateral sides. **(c)** Bar graphs show the percentage of PD-1$^-$ expression on CD4$^+$ TILs cells on the injected and contralateral sides. **(d)** Gating strategy for detection of CD44$^+$ and CD69$^+$ expression on CD8$^+$ CD3$^+$ and PD-1$^-$ CD8$^+$ TILs. **(e)** Gating strategy for detection of CD44$^+$ and CD69$^+$ expression on CD8$^+$ CD3$^+$ in TDLNs. **(f)** Bar graphs show the percentage of CD44$^+$ and CD69$^+$ on CD8$^+$ CD3$^+$ cells in TDLNs. Data are presented as mean ± SD (n=3 mice). **(g)** Gating strategy for detection of CD103$^+$ KLRG-1$^+$ expression on CD4$^+$ CD25$^+$ FOXP3$^+$ and bar graphs show the percentage of CD4$^+$ CD25$^+$ FOXP3$^+$ tumor-infiltrating T-reg cells on the injected and contralateral sides. (h) Bar graphs shows the ratio between CD44$^+$ CD8$^+$ PD-1$^-$ population and terminally differentiated CD103$^+$ KLRG-1$^+$ T-reg cells on the injected and contralateral sides **(i)** Gating strategy for detection of XCR-1 expression on cDC1 in tumor . Data are presented as mean ± SD (n=4 mice). This experiment was conducted at least two times . One-way ANOVA with a post-hoc Tukey's tests was performed.* $p < 0.05$, ** $p < 0.01$, *** $p < 0.001$, **** $p < 0.0001$.